PHYSICAL REVIEW B **95**, 060408(R) (2017)

Strength of effective Coulomb interactions and origin of ferromagnetism in hydrogenated graphene

E. Şaşıoğlu,[1,2] H. Hadipour,[3] C. Friedrich,[2] S. Blügel,[2] and I. Mertig[1]
[1]*Institut für Physik, Martin-Luther-Universität Halle-Wittenberg, D-06099 Halle (Saale), Germany*
[2]*Peter Grünberg Institut and Institute for Advanced Simulation, Forschungszentrum Jülich and JARA, 52425 Jülich, Germany*
[3]*Department of Physics, University of Guilan, 41335-1914 Rasht, Iran*
(Received 12 December 2016; published 15 February 2017)

Hydrogenation provides a novel way to tune the electronic properties of graphene. Recent scanning tunneling microscopy experiments have demonstrated that local graphene magnetism can be selectively switched on and off by hydrogen (H) dimers. Employing first-principles calculations in conjunction with the constrained random-phase approximation we determine the strength of the effective Coulomb interaction U in hydrogenated graphene. We find that the calculated U parameters are smaller than the ones in graphene and depend on the H concentration. Moreover, the U parameters are very sensitive to the position of H atoms adsorbed on the graphene lattice. We discuss the instability of the paramagnetic state of the hydrogenated graphene towards the ferromagnetic one on the basis of calculated U parameters within the Stoner model. Spin-polarized calculations reveal that the itinerant ferromagnetism in hydrogenated graphene can be well accounted for by the Stoner model.

DOI: 10.1103/PhysRevB.95.060408

After the experimental synthesis of graphene, much attention has been paid to the study of various properties of carbon allotropes [1,2]. Electronic and optical properties of graphene may drastically change by adsorption of atoms like hydrogen (H) on the graphene surface [3–5]. H atoms destroy the conelike dispersion of graphene and open a band gap in the single-particle spectrum. Fully hydrogenated graphene is referred to as graphane [5]. Hydrogenation provides a novel way to tune the properties of graphene with unprecedented potential for applications. From graphene to semihydrogenated graphene (graphone) and to graphane, the system evolves from a nonmagnetic metallic state to a ferromagnetic semiconductor and to a nonmagnetic insulator.

Magnetism is a very subtle issue in functionalized graphene and carbon-based materials. First-principles theoretical studies have predicted that adsorption of H atoms (chemisorption defects) or carbon vacancy defects in graphene yield the formation of magnetic moments and a long-range magnetic order [6–13]. In the partially hydrogenated graphene, the breaking of the π bonding network by adsorption of H gives rise to the formation of unpaired electrons in the C atoms in the sublattice opposite to the one where the H atoms are chemisorbed, which gives rise to the formation of magnetic moments if the Coulomb interaction is strong enough. Despite this clear theoretical picture of magnetism, its experimental evidence remained both scarce and controversial [14–22]. It has been experimentally demonstrated that point defects in graphene result in the appearance of spin-half paramagnetism [23,24]. Proton irradiation induces a ferromagnetic order in graphite [25]. In a recent STM study, Gonzales-Herrero *et al.* deposited a single H atom on top of graphene and detected magnetism on the sublattice lacking the deposited atom [26]. The scanning tunneling microscopy (STM) measurements also revealed the itinerant character of local magnetism, i.e., the spin polarization extends over several C sublattices. Moreover, the authors demonstrated the possibility of selectively switching the local magnetization on and off by the formation of different types of H dimers.

Different mechanisms have been proposed to account for the origin of magnetism in functionalized graphene and carbon-based materials [7,27–29]. A widely accepted concept is the Stoner model, in which the paramagnetic state is unstable towards ferromagnetism if the criterion $UN(E_F) > 1$ is satisfied where $N(E_F)$ is the density of states (DOS) at the Fermi energy E_F and U is the effective Coulomb interaction parameter. A numerical study of the Anderson-Hubbard Hamiltonian for graphene with defects gives a magnetic solution [27], and the behavior of the magnetization turns out to be strongly dependent on the effective Coulomb interaction U [27,28]. A complementary approach, the so-called flatband model, in which ferromagnetism occurs for any $U > 0$ due to the infinite DOS at the Fermi energy [10,13], is proposed to account for the magnetism in hydrogenated carbon-based materials [10,13]. In both models, the effective Coulomb interaction U plays a decisive role in the formation of magnetic moments and long-range magnetic order.

The aim of the present Rapid Communication is a first-principles determination of the effective Coulomb interaction U in hydrogenated graphene. The instability of the paramagnetic state toward ferromagnetism is discussed on the basis of the calculated U parameters within the Stoner model. Our constrained random-phase approximation (cRPA) calculations within the full-potential linearized augmented-plane-wave (FLAPW) method show that the calculated U parameters are smaller than the ones in pristine graphene and depend on the H concentration. Moreover, U parameters are very sensitive to the position of H atoms adsorbed on the graphene lattice. A comparison of the predictions of the Stoner model with spin-polarized density functional theory (DFT) calculations reveals that the Stoner model can account for the delocalized character of ferromagnetism in hydrogenated graphene in very good agreement with recent STM experiments as well as previous first-principles studies.

To simulate hydrogenated graphene, we consider the conventional hexagonal unit cell for graphone (containing two C atoms with a single H atom) and graphane (containing two C atoms with two H atoms) as well as a 3×3 supercell (see Fig. 1). The supercell contains an H impurity ($C_{18}H$) and H dimers with different H-H distances. The H dimers are denoted as AA (AB) if the H atoms are on the same (different) sublattice. For

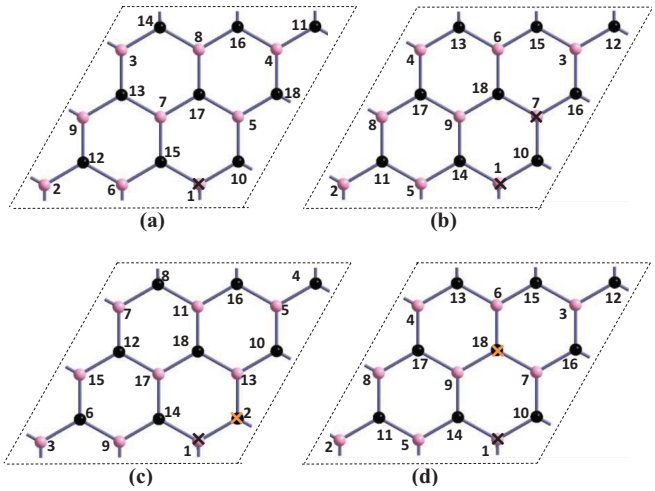

FIG. 1. The crystal structure of the two-dimensional 3×3 supercell with (a) a single H atom on sublattice A ($C_{18}H$); (b) an AA dimer [$C_{18}H_2$(nn)], H atoms are next-nearest neighbors; (c) an AB dimer [$C_{18}H_2$(n)], H atoms are nearest neighbors; and (d) an AB dimer [$C_{18}H_2$(nnn)], H atoms are next-next-nearest neighbors. Dark and light circles are carbon atoms in different sublattices. Circles with × denote carbon atoms bonded to H.

comparison, pristine graphene is also considered. Simulation of both unit cells is based on the slab model having a 25 Å vacuum separating them and the distortion of the lattice is taken into account. The latter is important to induce a spin polarization in hydrogenated graphene [30].

The DFT calculations are carried out with the FLEUR code, which is based on an FLAPW implementation [31]. The generalized gradient approximation [32] for the exchange-correlation energy functional is adopted. We use an 8×8×1 k-point grid for the 3×3 supercell, while a dense 24×24×1 k-point grid is used for the small unit cell of graphone and graphane. For the plane waves we use a linear momentum cutoff of $G_{\max} = 4.5$ bohrs^{-1}. The DFT calculations are used as an input for the SPEX code [33] to perform cRPA calculations for the effective Coulomb interaction parameters (Hubbard U) [34–36]. The SPEX code uses the WANNIER90 library to construct the maximally localized Wannier functions for the p_z orbitals of the C atoms in hydrogenated graphene [37,38]. For this construction, we use ten states per C atom. Dense 18×18×1 and 6×6×1 k-point grids are used in the cRPA calculations of the small unit cell and 3×3 supercell, respectively. The cRPA method offers an efficient way to calculate the effective Coulomb interaction parameter U and allows one to determine individual Coulomb matrix elements, e.g., on-site, off-site, interorbital, intraorbital, as well as their frequency dependence.

We begin with the discussion of the local (on-site) and nonlocal (off-site) effective Coulomb interaction parameters U for graphone and graphane. For comparison, the corresponding U values for pristine graphene are also calculated. The results are presented in Table I. In graphane and graphene, the screening is weak and we obtain comparatively large U values, the one of the former being about 1 eV larger due to the existence of the band gap. It is worth noting that in two-dimensional semiconductors and insulators the screening is nonconventional, i.e., at intermediate distances the Coulomb interaction is weakly screened, while at large distances it is unscreened. Due to this nonconventional screening the calculated off-site U parameters for graphane and graphene (see Table I) turn out to be rather sizable [39–42]. On the other hand, the situation is different in the case of graphone due to the existence of metallic p_z states around the Fermi energy. The $p_z \to \sigma$ screening channel substantially contributes to the polarization function and, as a consequence, the calculated U values are considerably smaller than the corresponding values in graphane and graphene. Moreover, the off-site U values in graphone are strongly screened. Note also that for graphone the U values presented in Table I are for the non-spin-polarized case. The variation of U in spin-polarized calculations amounts to about 0.1 eV. The appearance of magnetism in graphone and partially hydrogenated graphene will be discussed in detail below.

TABLE I. On-site (U^A_{00}, U^B_{00}), nearest-neighbor (U_{01}), next-nearest-neighbor (U^A_{02}, U^B_{02}), and third-nearest-neighbor (U_{03}) Coulomb interaction parameters for graphene, graphone, and graphane. In graphene and graphane $U^A_{00} = U^B_{00}$ and $U^A_{02} = U^B_{02}$ due to the sublattice symmetry. The bare and partially screened cRPA (Hubbard U) parameters are given for p_z orbitals (sp^3 orbitals in the case of graphane).

	Graphene		Graphone		Graphane	
	Bare	cRPA	Bare	cRPA	Bare	cRPA
$U^{A/B}_{00}$	16.7	8.7	16.6, 16.5	4.3, 2.5	16.5	9.8
U_{01}	8.5	4.0	8.2	0.6	8.7	5.3
$U^{A/B}_{02}$	5.4	2.5	5.2, 5.2	0.3, 0.3	5.7	3.7
U_{03}	4.7	2.2	4.6	0.2	4.9	3.3

The calculation of the frequency dependence of the effective Coulomb interaction $U(\omega)$ reveals that the strong screening of U in graphone takes place only at low frequencies. As seen in Fig. 2(a) the on-site $U_{00}(\omega)$ increases linearly and at about $\omega = 2.5$ eV it reaches the static value (9 eV) of graphene and graphane. In the latter, $U(\omega)$ shows a smooth behavior at low frequencies (up to 5 eV). The strong frequency dependence of

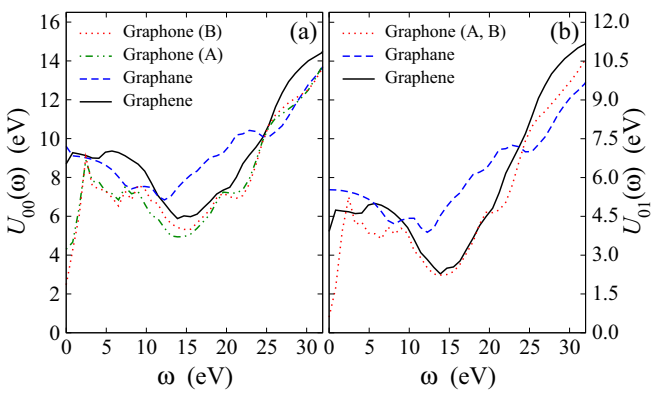

FIG. 2. Frequency dependence of the (a) on-site $U_{00}(\omega)$ and (b) nearest-neighbor $U_{01}(\omega)$ effective Coulomb interaction for graphene, graphone, and graphane.

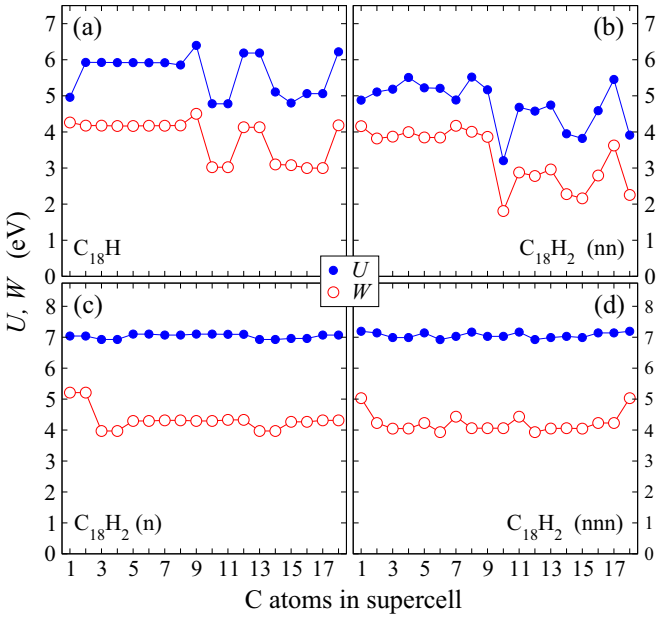

FIG. 3. Calculated partially screened U and fully screened W Coulomb interaction parameters for C $2p_z$ electrons in the cases of (a) a single H atom on sublattice A ($C_{18}H$), (b) AA dimer [$C_{18}H_2$(nn)], (c) AB dimer [$C_{18}H_2$(n)] with nearest-neighbor separation, and (d) AB dimer [$C_{18}H_2$(nnn)] with next-next-nearest-neighbor separation (see Fig. 1).

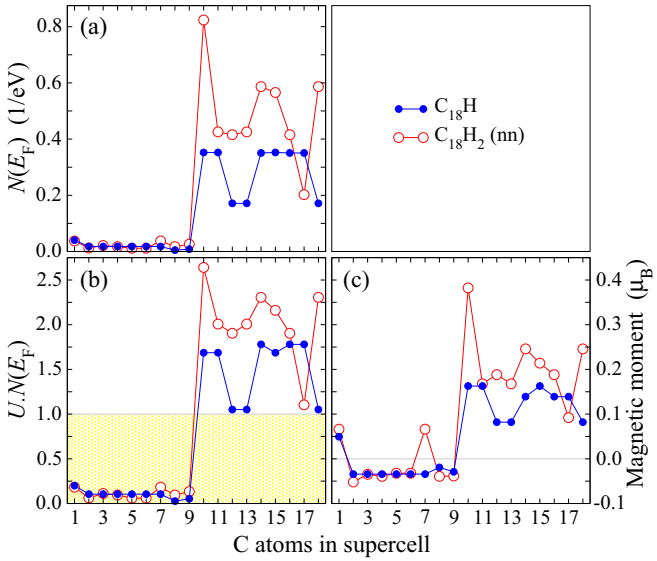

FIG. 4. (a) DOS at the Fermi level for the nonmagnetic case, (b) Stoner criterion, and (c) magnetic moments (in μ_B) of different carbon atoms in the case of a single H atom on A sublattice ($C_{18}H$) and the AA dimer [$C_{18}H_2$(nn)]. C atoms 1 to 9 (10 to 18) belong to the sublattice A (B).

$U(\omega)$ in graphone stems from the efficient screening involving the p_z states close to the Fermi level, which form a bandwidth of about 2.5 eV (not shown). For frequencies larger than 2.5 eV the behavior of $U(\omega)$ for all three systems is similar. The situation is not different for the off-site [nearest-neighbor $U_{01}(\omega)$] Coulomb interaction shown in Fig. 2(b). It is worth noting that due to the strong variation of the effective Coulomb interaction for graphone at low frequencies the use of the static $U(\omega = 0)$ in model Hamiltonian studies may be inappropriate.

In the following, we will consider partially hydrogenated graphene with a single H atom ($C_{18}H$) as well as AA and AB (H) dimers ($C_{18}H_2$) per 3×3 supercell. In addition to the partially screened interaction parameters U we also report the respective fully screened interaction parameters W. We note that the systems with AB dimers are semiconducting, while the others are metallic in constrained non-spin-polarized DFT calculations. The obtained U and W parameters are presented in Fig. 3 (see Fig. 1 for H-atom configurations). Generally, partial hydrogenation of the graphene sheet reduces the Coulomb matrix elements compared to pristine graphene. This reduction is not substantial in the case of semiconducting AB dimers and the calculated U (W) values turn out to be around 7 eV (4–5 eV) for all C atoms [Figs. 3(c) and 3(d)], while for the metallic systems the reduction of U and W is much more pronounced [Figs. 3(a) and 3(b)]. The obtained U (W) parameters vary in the range 3.2–6.2 eV (1.8–4.5 eV). Moreover, the U and W parameters for the C atoms [10 to 18 in Figs. 3(a) and 3(b)] on the sublattice opposite to the one where the H atom is chemisorbed show strong variations. These variations stem from different densities of p_z states of the corresponding C atoms at the Fermi energy, shown in Fig. 4(a). As seen, the carbon atoms (1 to 9) that are located in the sublattice where the H atom is adsorbed indeed hardly contribute to the DOS at E_F, while the carbon atoms in the other sublattice contribute significantly with large variation from atom to atom. The large $U - W$ differences both in metallic and semiconducting systems reveal a strong contribution of the p_z states around the Fermi energy to the screening through $p_z \rightarrow p_z$ transitions.

We now return to the discussion of the appearance of ferromagnetism in partially hydrogenated graphene. The mean-field (Hartree-Fock) solution of the Hubbard model leads to the so-called Stoner criterion, which states that the system becomes ferromagnetic when the condition $UN(E_F) > 1$ is satisfied, where $N(E_F)$ is the DOS at the Fermi energy of the corresponding non-spin-polarized system. Although the Stoner criterion has been derived for a model system, it can serve as a guide to search for ferromagnetism in systems in which the U parameter or the DOS at the Fermi energy is large. On the other hand, there might be systems with low electron densities which fully satisfy the Stoner criterion but which do not exhibit ferromagnetism [43,44], e.g., flatband Hubbard models. In Hubbard model studies of partially hydrogenated graphene, it was shown that one needs a U value of at least 3 eV to get a ferromagnetic ground state [8,9]. Our calculated U parameters presented in Fig. 3 range between 3.2 and 6.2 eV, large enough to induce ferromagnetism in hydrogenated graphene. Note that for AB dimers due to Lieb's theorem [45] the ground state is expected to be either nonmagnetic or antiferromagnetic with zero total magnetic moment. Thus, we will focus only on the instability of the paramagnetic state towards ferromagnetism for an AA dimer and for a single H atom in the graphene lattice. In Figs. 4(a) and 4(b) we present the DOS at the Fermi energy $N(E_F)$ for the non-spin-polarized case and the Stoner criterion $UN(E_F)$,

respectively. As seen, in both cases only the C atoms in the sublattice that is free of adsorbed H atoms satisfy the Stoner criterion $UN(E_F) > 1$ due to the large DOS $N(E_F)$ at the Fermi energy and, as a result, the ground state is expected to be unstable towards ferromagnetism and the C atoms that satisfy the criterion would present a net magnetic moment.

Indeed, our spin-polarized DFT calculations show exactly that; only those C atoms that satisfy the Stoner criterion exhibit sizable magnetic moments, as presented in Fig. 4(c), while the other C atoms only show a small induced negative spin magnetic moment. The calculated magnetization is rather delocalized with a total spin magnetic moment of $1\mu_B$ for a single H atom and $2\mu_B$ for the AA dimer in good agreement with recent experiments and previous first-principles studies [27,29]. In the case of AB dimers [$C_{18}H_2$(n) and $C_{18}H_2$(nnn)] our spin-polarized DFT calculations yield a nonmagnetic semiconducting ground state in accordance with Lieb's theorem as well as previous studies [4,46]. We now return to the discussion of the magnetism in graphone, which shows similar behavior. The C atoms that are not bound to H satisfy the Stoner criterion because of the large DOS at the Fermi level $N(E_F) = 0.591/\text{eV}$ and thus, the spin-polarized calculations result in a ferromagnetic semiconducting ground state with a large magnetic moment of about $1\mu_B$ per unit cell.

Theoretical predictions of ferromagnetism in hydrogenated graphene were recently confirmed by STM experiments. Gonzales-Herrero *et al.* demonstrated that the adsorption of a single H atom on graphene induces a magnetic moment characterized by a ∼20 meV spin-split state at the Fermi energy [26]. It was shown that such a spin-polarized state is essentially localized on the carbon sublattice opposite to the one where the H atom is chemisorbed and extends several nanometers away from the H atom. By using the STM tip the authors manipulated the H atoms with atomic precision and demonstrated the possibility of selectively switching the local magnetization on and off by changing the H dimers from AA to AB. The detected magnetism persists for AA dimers with an H-H separation of 1.5 nm and disappears for the AB dimer with similar separation. The observed experimental picture of ferromagnetism in hydrogenated graphene is fully supported by first-principles DFT calculations [26]. The success of DFT in low-dimensional systems can be attributed to the nonconventional screening of the Coulomb interaction mentioned above, which reduces the gradient of the Coulomb interaction and, as a consequence, makes local and semilocal approximations to the exchange-correlation potential appropriate [39–42].

In conclusion, we have determined the strength of the effective Coulomb interaction U in hydrogenated graphene by employing first-principles calculations in conjunction with the cRPA method. We have found that the calculated U parameters are smaller than the ones in pristine graphene and depend on the H concentration. Moreover, the U parameters are very sensitive to the position of H atoms adsorbed on the graphene lattice. On the basis of the calculated U parameters, we have discussed the instability of the paramagnetic state of hydrogenated graphene towards ferromagnetism within the Stoner model. It has been deduced that only the adsorption of a single H atom or of H dimers where the two H atoms are bound to the same carbon sublattice can give rise to magnetic instability, which we have confirmed by spin-polarized DFT calculations. On the other hand, the adsorption of dimers of H atoms that adsorb on different sublattices produces a semiconducting ground state in agreement with Lieb's theorem and with STM experiments. The itinerant ferromagnetism in hydrogenated graphene can be well explained by the Stoner model. The U parameters are not only important for a fundamental understanding of ferromagnetism in hydrogenated graphene. They can also serve as effective interaction parameters to be used in model Hamiltonians applied to describe electronic, optical, and magnetic properties. This provides model parameters from first principles rather than having to fit them to experimental data, thus increasing the predictive power of model calculations.

[1] A. K. Geim and K. S. Novoselov, Nat. Mater. **6**, 183 (2007).
[2] M. I. Katsnelson, Mater. Today **10**, 20 (2007).
[3] J. O. Sofo, A. S. Chaudhari, and G. D. Barber, Phys. Rev. B **75**, 153401 (2007).
[4] D. W. Boukhvalov, M. I. Katsnelson, and A. I. Lichtenstein, Phys. Rev. B **77**, 035427 (2008).
[5] D. C. Elias, R. R. Nair, T. M. G. Mohiuddin, S. V. Morozov, P. Blake, M. P. Halsall, A. C. Ferrari, D. W. Boukhvalov, M. I. Katsnelson, A. K. Geim *et al.*, Science **323**, 610 (2009).
[6] J. Zhou, Q. Wang, Q. Sun, X. S. Chen, Y. Kawazoe, and P. Jena, Nano Lett. **9**, 3867 (2009).
[7] O. V. Yazyev and L. Helm, Phys. Rev. B **75**, 125408 (2007).
[8] O. V. Yazyev, Rep. Prog. Phys. **73**, 056501 (2010).
[9] O. V. Yazyev, Phys. Rev. Lett. **101**, 037203 (2008).
[10] K. Seki, T. Shirakawa, Q. Zhang, T. Li, and S. Yunoki, Phys. Rev. B **93**, 155419 (2016).
[11] J. J. Palacios, J. Fernández-Rossier, and L. Brey, Phys. Rev. B **77**, 195428 (2008).
[12] A. N. Rudenko, F. J. Keil, M. I. Katsnelson, and A. I. Lichtenstein, Phys. Rev. B **88**, 081405(R) (2013).
[13] X. Yang and G. Wu, ACS Nano **3**, 1646 (2009).
[14] Y. Wang, Y. Huang, Y. Song, X. Zhang, Y. Ma, J. Liang, and Y. Chen, Nano Lett. **9**, 220 (2009).
[15] H. S. S. Ramakrishna Matte, K. S. Subrahmanyam, and C. N. R. Rao, J. Phys. Chem. C **113**, 9982 (2009).
[16] M. Sepioni, R. R. Nair, S. Rablen, J. Narayanan, F. Tuna, R. Winpenny, A. K. Geim, and I. V. Grigorieva, Phys. Rev. Lett. **105**, 207205 (2010).
[17] A. Ney, P. Papakonstantinou, A. Kumar, N. G. Shang, and N. Peng, Appl. Phys. Lett. **99**, 102504 (2011).
[18] S. C. Ray, N. Soin, T. Makgato, C. H. Chuang, W. F. Pong, S. S. Roy, S. K. Ghosh, A. Strydom, and J. A. Mclaughlin, Sci. Rep. **4**, 3862 (2014).
[19] J. Barzola-Quiquia, P. Esquinazi, M. Rothermel, D. Spemann, T. Butz, and N. Garcia, Phys. Rev. B **76**, 161403 (2007).
[20] H. Ohldag, T. Tyliszczak, R. Höhne, D. Spemann, P. Esquinazi, M. Ungureanu, and T. Butz, Phys. Rev. Lett. **98**, 187204 (2007).
[21] R. R. Nair, I.-L. Tsai, M. Sepioni, O. Lehtinen, J. Keinonen, A. V. Krasheninnikov, A. H. Castro Neto, M. I. Katsnelson, A. K. Geim, and I. V. Grigorieva, Nat. Commun. **4**, 2010 (2013).

[22] J. S. Caronervenka, M. I. Katsnelson, and C. F. J. Flipse, Nat. Phys. **5**, 840 (2009).
[23] R. R. Nair, M. Sepioni, I-Ling Tsai, O. Lehtinen, J. Keinonen, A. V. Krasheninnikov, T. Thomson, A. K. Geim, and I. V. Grigorieva, Nat. Phys. **8**, 199 (2012).
[24] Y. Zhang, S.-Y. Li, H. Huang, W.-T. Li, J.-B. Qiao, W.-X. Wang, L.-J Yin, K.-K. Bai, W. Duan, and L. He, Phys. Rev. Lett. **117**, 166801 (2016).
[25] P. Esquinazi, D. Spemann, R. Hohne, A. Setzer, K.-H. Han, and T. Butz, Phys. Rev. Lett. **91**, 227201 (2003).
[26] H. González-Herrero, J. M. Gómez-Rodríguez, P. Mallet, M. Moaied, J. J. Palacios, C. Salgado, M. M. Ugeda, J.-Y. Veuillen, F. Yndurain, and I. Brihuega, Science **352**, 437 (2016).
[27] J. O. Sofo, Gonzalo Usaj, P. S. Cornaglia, A. M. Suarez, A. D. Hernández-Nieves, and C. A. Balseiro, Phys. Rev. B **85**, 115405 (2012).
[28] H. Kumazaki and D. S. Hirashima, J. Phys. Soc. Jpn. **76**, 064713 (2007).
[29] H.-Y. Lu, L. Hao, R. Wang, and C. S. Ting, Phys. Rev. B **93**, 241410(R) (2016).
[30] S. Casolo, E. Flage-Larsen, O. M. Løvvik, G. R. Darling, and G. F. Tantardini, Phys. Rev. B **81**, 205412 (2010).
[31] See http://www.flapw.de.
[32] J. P. Perdew, K. Burke, and M. Ernzerhof, Phys. Rev. Lett. **77**, 3865 (1996).
[33] C. Friedrich, S. Blügel, and A. Schindlmayr, Phys. Rev. B **81**, 125102 (2010).
[34] F. Aryasetiawan, M. Imada, A. Georges, G. Kotliar, S. Biermann, and A. I. Lichtenstein, Phys. Rev. B **70**, 195104 (2004); F. Aryasetiawan, K. Karlsson, O. Jepsen, and U. Schönberger, *ibid.* **74**, 125106 (2006); T. Miyake, F. Aryasetiawan, and M. Imada, *ibid.* **80**, 155134 (2009); I. V. Solovyev, J. Phys.: Condens. Matter **20**, 293201 (2008).
[35] E. Şaşıoğlu, C. Friedrich, and S. Blügel, Phys. Rev. B **83**, 121101(R) (2011); T. O. Wehling, E. Şaşıoğlu, C. Friedrich, A. I. Lichtenstein, M. I. Katsnelson, and S. Blügel, Phys. Rev. Lett. **106**, 236805 (2011); E. Şaşıoğlu, C. Friedrich, and S. Blügel, *ibid.* **109**, 146401 (2012).
[36] Y. Nomura, M. Kaltak, K. Nakamura, C. Taranto, S. Sakai, A. Toschi, R. Arita, K. Held, G. Kresse, and M. Imada, Phys. Rev. B **86**, 085117 (2012); B-C. Shih, Y. Zhang, W. Zhang, and P. Zhang, *ibid.* **85**, 045132 (2012).
[37] A. A. Mostofi, J. R. Yates, Y.-S. Lee, I. Souza, D. Vanderbilt, and N. Marzari, Comput. Phys. Commun. **178**, 685 (2008).
[38] F. Freimuth, Y. Mokrousov, D. Wortmann, S. Heinze, and S. Blügel, Phys. Rev. B **78**, 035120 (2008).
[39] J. van den Brink and G. A. Sawatzky, Europhys. Lett. **50**, 447 (2000).
[40] J. Deslippe, M. Dipoppa, D. Prendergast, M. V. O. Moutinho, R. B. Capaz, and S. G. Louie, Nano Lett. **9**, 1330 (2009).
[41] P. Cudazzo, I. V. Tokatly, and A. Rubio, Phys. Rev. B **84**, 085406 (2011).
[42] M. van Schilfgaarde and M. I. Katsnelson, Phys. Rev. B **83**, 081409(R) (2011).
[43] H. Tasaki, Phys. Rev. Lett. **69**, 1608 (1992).
[44] A. Mielke and H. Tasaki, Commun. Math. Phys. **158**, 341 (1993).
[45] E. H. Lieb, Phys. Rev. Lett. **62**, 1201 (1989).
[46] A. Ranjbar, M. S. Bahramy, M. Khazaei, H. Mizuseki, and Y. Kawazoe, Phys. Rev. B **82**, 165446 (2010).